

Enhancement of the Large Stokes-Shifted Fluorescence Emission from the 2-(2'-Hydroxyphenyl)benzoxazole Core in a Dendrimer

Asuka Ohshima,[†] Atsuya Momotake,[†] Ritsuko Nagahata,[‡] and Tatsuo Arai^{*†}

Graduate School of Pure and Applied Sciences, University of Tsukuba, 1-1-1 Tennodai, Tsukuba-city, Ibaraki 305-8571, and Research Center of Macromolecular Technology, National Institute of Advanced Industrial Science and Technology (AIST), Tsukuba City, Ibaraki 305-8565, Japan

Received: July 7, 2005; In Final Form: September 5, 2005

The photochemical properties of a series of newly synthesized dendrimers, **4–6**, having a 2-(2'-hydroxyphenyl)-benzoxazole (HBO) core, were studied in benzene. The fluorescence quantum yields (Φ_f) were determined to be 0.022, 0.030, and 0.038 for **4**, **5**, and **6**, respectively, increasing in higher generation dendrimers. With transient absorption spectroscopy, the quantum yields of the isomerization from the (*E*)-keto form ($^1K_E^*$) to the (*Z*)-keto form (1K_Z) ($\Phi_{E\rightarrow Z}$) and those of intersystem crossing (Φ_{isc}) can be estimated. Whereas $\Phi_{E\rightarrow Z}$ values decreased in higher generation dendrimers, Φ_{isc} values were almost the same among **4–6**. The quantum yields of nonradiative decay (Φ_{nr}) increased in higher generation dendrimers. The dendrimer structure also affected the reverse tautomerization process.

Introduction

Molecules with intramolecular hydrogen bonds often exhibit excited-state intramolecular proton (or hydrogen atom) transfer (ESIPT) and have attracted considerable research interest from the viewpoint of the development of new functional molecules, such as fluorescent metal probes,¹ laser dyes,² and photostabilizers.³ ESIPT is a photochemical tautomerization that yields an excited keto form (K^*) from the original enol form (*E*) in the subpicosecond time region.⁴ The excited-state keto form relaxes radiatively to give a fluorescence spectrum with a large Stokes shift or nonradiatively to the ground-state keto form, which undergoes thermal re-enolization to give the stable enol form.⁵ The large Stokes-shifted fluorescence due to ESIPT has an attractive character of unusual emission at longer wavelength from a small molecule and therefore is not reabsorbed even in a high concentration of chromophores. Despite such a unique character, the efficiency of the large Stokes-shifted fluorescence is generally low⁶ partially due to the deactivation by isomerization from the excited-state tautomer. When a large substituent is introduced to the molecule, the isomerization efficiency from the excited state may be diminished because a much larger volume change should be required for the deactivation process. We considered that the suppression of the isomerization efficiency in ESIPT molecules may lead to an increase in the efficiency of the large Stokes-shifted fluorescence. A dendritic structure can be one of the good candidates for this approach. A dendritic structure may also avoid the bimolecular quenching of the fluorescent core in the excited state.⁷ There is no report about the dendrimer effect on the photochemical behaviors of the ESIPT molecules in solution.

2-(2'-Hydroxyphenyl)benzoxazole (HBO) is known as one of the typical molecules exhibiting ESIPT.⁸ On direct irradiation, the enol form (*E*) of HBO undergoes ESIPT to give the excited

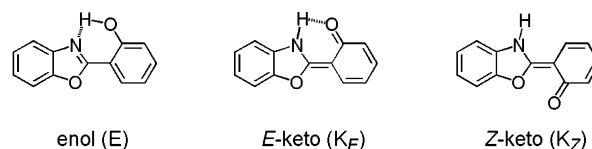


Figure 1. Chemical structures of HBO and its tautomers: enol form (*E*), (*E*)-keto form (K_E), and (*Z*)-keto form (K_Z).

keto form (K^*) (Figure 1). When HBO is surrounded by the dendron group, one can expect an increase of the stability of the reactive intermediate and a decrease of the bimolecular quenching rate constant. We report here the synthesis of dendrimers with photoreactive hydrogen-bonded chromophores and the dendrimer effect on the fluorescence quantum yield and the lifetime of the intermediate tautomer.

Experimental Section

Materials. Compounds **1–6** were prepared according to the procedure given in Scheme 1).

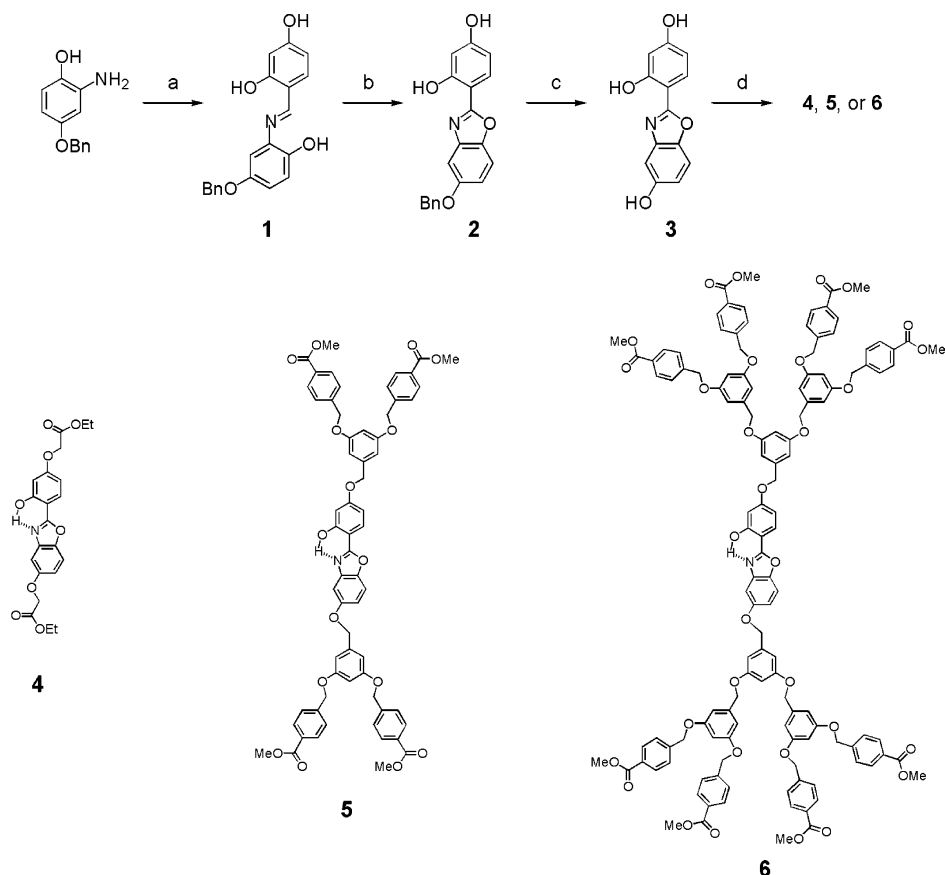
4-[(5-Benzyloxy-2-hydroxyphenylimino)methyl]benzene-1,3-diol (1). 5-Benzyloxy-2-hydroxyaniline was prepared from 4-benzyloxy-2-nitrophenol (245 mg, 1.0 mmol)⁹ by reduction with a catalytic amount of Pt-C (22 mg) under H_2 in ethanol (20 mL). After filtration to remove the catalyst, the aniline in ethanol was immediately added to a solution of 2,5-dihydroxybenzaldehyde (138 mg, 1.0 mmol) in ethanol (10 mL) and was refluxed for 2 h. After evaporation, the yellow solid residue was recrystallized from hexane/ethyl acetate (2:1) to give Schiff base **1** as a yellow solid (280 mg, 0.82 mmol, 82%): 1H NMR (400 MHz, $CDCl_3$, Me_4Si) δ 9.64 (s, 1H, $CH=N$), 8.44 (d, 2H, $J = 7.6$ Hz, ArH), 8.36 (t, 1H, $J = 7.6$ Hz, ArH), 8.30 (d, 1H, $J = 6.8$ Hz, ArH), 8.24 (d, 1H, $J = 8.8$ Hz, ArH), 7.84 (d, 1H, $J = 8.8$ Hz, ArH), 7.76 (d, 1H, $J = 8.8$ Hz, ArH), 7.23 (d, 1H, $J = 8.8$ Hz, ArH), 6.05 (s, 2H, ArH).

4-(5-Benzyloxybenzoxazol-2-yl)benzene-1,3-diol (2). A mixture of DDQ (540 mg) and **1** (210 mg, 0.63 mmol) in dichloromethane (5 mL) was stirred at room temperature for 1 h. After the mixture was concentrated in vacuo, the black residue

* To whom correspondence should be addressed. Fax: +81-298-53-6503. E-mail: arai@chem.tsukuba.ac.jp.

[†] University of Tsukuba.

[‡] National Institute of Advanced Industrial Science and Technology.

SCHEME 1^a

^a Reagents and conditions: (a) 2,5-dihydroxybenzaldehyde, ethanol, reflux, 2 h; (b) DDQ, dichloromethane, room temperature, 1 h; (c) H₂, Pd–C, acetic acid, room temperature, 3 days; (d) *Gn*-Br, K₂CO₃, 18-crown-6-ether, acetone, reflux, 28–43 h.

was purified by silica gel column chromatography [hexane/ethyl acetate (10:0 → 3:1)], followed by recrystallization from chloroform, yielding **2** as a white solid (29 mg, 87 μmol, 13%): ¹H NMR (400 MHz, CDCl₃, Me₄Si) δ 8.81 (d, 1H, *J* = 8.8 Hz, ArH), 8.50 (d, 1H, *J* = 8.8 Hz, ArH), 8.46 (d, 2H, *J* = 7.6 Hz, ArH), 8.37 (t, 2H, *J* = 7.6 Hz, ArH), 8.31 (d, 1H, *J* = 7.6 Hz, ArH), 8.28 (s, 1H, ArH), 8.20 (d, 1H, *J* = 7.6 Hz, ArH), 7.47 (d, 1H, *J* = 7.6 Hz, ArH), 7.43 (s, 1H, ArH), 6.13 (s, 2H, ArH).

4-(5-Hydroxybenzoxazol-2-yl)benzene-1,3-diol (3). A mixture of **2** (265 mg, 0.79 mmol) and 10% Pd–C (20 mg) in acetic acid was stirred at room temperature under H₂ for 3 days. The mixture was filtrated, washed with ethyl acetate, and concentrated in vacuo. The residue was purified on silica gel [hexane/ethyl acetate (10:0 → 3:1)], providing **3** as a white solid (160 mg, 0.66 mmol, 83%): ¹H NMR (400 MHz, CDCl₃, Me₄Si) δ 7.72 (d, 1H, *J* = 8.8 Hz, ArH), 7.32 (d, 1H, *J* = 8.8 Hz, ArH), 6.93 (s, 1H, ArH), 6.72 (dd, 1H, *J* = 8.8 and 2.4 Hz, ArH), 6.38 (dd, 1H, *J* = 8.8 and 2.4 Hz, ArH), 6.34 (1H, *J* = 2.4 Hz, ArH).

Compound 4. A mixture of **3** (60 mg, 0.25 mmol), K₂CO₃ (85 mg, 0.61 mmol), 18-crown-6 ether (10 mg), and ethyl bromoacetate (83 mg, 0.50 mmol) in dry acetone (20 mL) was refluxed under nitrogen for 28 h. After evaporation to dryness, the residue was dissolved in dichloromethane and washed with water. The organic layer was dried over MgSO₄, filtered, and concentrated. The mixture was purified by silica gel column chromatography [dichloromethane/ether (10:0 → 9:1)] and by recrystallization from ethyl acetate to give **4** as a white solid (45 mg, 0.11 mmol, 45%): ¹H NMR (400 MHz, CDCl₃, Me₄Si) δ 11.58 (s, 1H, OH), 7.91 (d, 1H, *J* = 8.8 Hz, ArH), 7.47 (d,

1H, *J* = 8.8 Hz, ArH), 7.16 (d, 1H, *J* = 2.4 Hz, ArH), 7.01 (dd, 1H, *J* = 8.8 and 2.4 Hz, ArH), 6.63 (dd, 1H, *J* = 8.8 and 2.4 Hz, ArH), 6.58 (d, 1H, *J* = 2.4 Hz, ArH), 4.68 (s, 4H, OCH₂), 4.30 (q, 4H, *J* = 6.0 Hz, CO₂CH₂), 1.32 (t, 6H, *J* = 6.0 Hz, CH₃); ¹³C NMR (125 MHz, CDCl₃, Me₄Si) δ 168.8, 168.2, 163.9, 162.1, 160.5, 155.8, 144.2, 140.9, 128.4, 113.9, 110.8, 108.0, 104.7, 103.5, 102.0, 66.3, 65.2, 61.6, 61.5, 14.18, 14.15; ESI-MS *m/z* calcd for C₂₁H₂₂NO₈ 415.1345, found 416.0685 (M + H). Anal. Calcd for C₂₁H₂₁NO₈: C, 60.72; H, 5.10; N, 3.37. Found: C, 60.61; H, 5.32; N, 3.27.

Compound 5. A mixture of **3** (40 mg, 0.17 mmol), K₂CO₃ (57 mg, 0.41 mmol), 18-crown-6 ether (5 mg), and G2-Br (164 mg, 0.33 mmol) in dry acetone (25 mL) was refluxed under nitrogen for 43 h. After evaporation to dryness, the residue was dissolved in dichloromethane and washed with water. The organic layer was dried over MgSO₄, filtered, and concentrated. The mixture was purified by silica gel column chromatography [dichloromethane/ether (10:0 → 9:1)] and by recrystallization from ethyl acetate to give **5** as a white solid (50 mg, 59 μmol, 36%): ¹H NMR (400 MHz, CDCl₃, Me₄Si) δ 11.54 (s, 1H, OH), 8.03 (dd, 8H, *J* = 8.0 and 2.4 Hz, ArH), 7.87 (d, 1H, *J* = 8.8 Hz, ArH), 7.48 (d, 8H, *J* = 8.0 Hz, ArH), 7.43 (d, 1H, *J* = 8.8 Hz, ArH), 7.18 (d, 1H, *J* = 2.4 Hz, ArH), 6.96 (dd, 1H, *J* = 8.8 and 2.4 Hz, ArH), 6.69 (d, 2H, *J* = 2.4 Hz, ArH), 6.67 (d, 2H, *J* = 2.4 Hz, ArH), 6.64 (d, 1H, *J* = 2.4 Hz, ArH), 6.61 (d, 1H, *J* = 8.4 Hz, ArH), 6.55 (t, 2H, *J* = 2.4 Hz, ArH), 5.11 (s, 8H, OCH₂), 5.05 (s, 4H, OCH₂), 3.91 (s, 12H, OCH₃); ¹³C NMR (125 MHz, CDCl₃, Me₄Si) δ 166.8, 163.9, 163.0, 160.5, 159.9, 156.4, 143.8, 141.9, 141.8, 140.9, 139.5, 139.0, 129.9, 129.7, 128.2, 127.0, 113.8, 110.6, 108.2, 106.4, 104.2, 103.4, 102.2, 101.8, 101.7, 70.6, 69.8, 69.5, 52.1; MALDI-TOFMS

m/z calcd for $C_{63}H_{54}NO_{16}$ 1080.3, found 1080.2 (M + H). Anal. Calcd for $C_{63}H_{53}NO_{16}$: C, 70.06; H, 4.95; N, 1.30. Found: C, 69.67; H, 4.98; N, 1.17.

Compound 6. A mixture of **3** (100 mg, 0.46 mmol), K_2CO_3 (280 mg, 2.02 mmol), 18-crown-6 ether (15 mg), and G3-Br (850 mg, 0.93 mmol) in dry acetone (25 mL) was refluxed under nitrogen for 43 h. After evaporation to dryness, the residue was dissolved in dichloromethane and washed with water. The organic layer was dried over $MgSO_4$, filtered, and concentrated. The mixture was purified by silica gel column chromatography [dichloromethane/ether (10:0 \rightarrow 9:1)] and by GPC to give **6** as a white solid (200 mg, 97 μ mol, 24%): 1H NMR (400 MHz, $CDCl_3$, Me_4Si) δ 11.56 (s, 1H, OH), 8.02 (d, 16H, $J = 8.0$ Hz, ArH), 7.82 (d, 1H, $J = 8.8$ Hz, ArH), 7.45 (d, 16H, $J = 8.0$ Hz, dendron ArH), 7.39 (d, 1H, $J = 8.8$ Hz, ArH), 7.17 (d, 1H, $J = 2.4$ Hz, ArH), 6.95 (dd, 1H, $J = 8.8$ and 2.4 Hz, ArH), 6.62–6.69 (m, 13H, ArH), 6.60 (dd, 1H, $J = 8.8$ and 2.4 Hz, ArH), 6.52 (s, 6H, ArH), 5.08 (s, 16H, OCH_2), 5.04 (d, 4H, $J = 6.8$ Hz, OCH_2), 4.98 (s, 8H, OCH_2), 3.91 (s, 24H, CH_3); ^{13}C NMR (125 MHz, $CDCl_3$, Me_4Si) δ 166.8, 163.1, 160.1, 160.0, 159.9, 156.2, 141.9, 139.4, 139.3, 138.8, 130.1, 129.9, 129.8, 128.2, 127.0, 113.9, 110.6, 108.3, 106.4, 106.3, 104.2, 103.5, 102.3, 101.7, 101.6, 96.1, 70.7, 69.9, 69.4, 52.2; MALDI-TOFMS m/z calcd for $C_{127}H_{109}NO_{32}Na$ 2182.7, found 2182.4 (M + Na). Anal. Calcd for $C_{127}H_{109}NO_{32} \cdot 2H_2O$: C, 69.42; H, 5.18; N, 0.64. Found: C, 69.76; H, 5.15; N, 0.64.

Measurements. The 1H and ^{13}C NMR spectra were measured with Bruker ARX-400 (400 MHz for 1H NMR) and Bruker AVANCE 500 (125 MHz for ^{13}C NMR) spectrometers in a solution of $CDCl_3$ with tetramethylsilane as an internal standard. The UV absorption and fluorescence spectra were recorded on a Shimadzu UV-1600 UV-vis spectrophotometer and on a Hitachi F-4500 fluorescence spectrometer, respectively. Fluorescence lifetimes were determined with a Horiba NAES-1100 time-resolved spectrofluorometer. Laser flash photolyses were performed by using an excimer laser (Lambda Physik LPX-100, 308 nm, 20 ns fwhm) as the excitation light source, and a pulsed xenon arc (Ushio UXL-159) was used as a monitoring light source. A photomultiplier (Hamamatsu R-928) and a storage oscilloscope (Iwatsu TS-123) were used for detection.

Results and Discussion

Synthesis. Scheme 1 depicts the synthetic procedures for the series of dendrimers **4–6**. 5-Benzyloxy-2-hydroxyaniline was prepared from 4-benzyloxy-2-nitrophenol⁹ by reduction with a catalytic amount of Pt-C under H_2 in ethanol, which was treated with an aldehyde to give Schiff base **1**, followed by oxidation of **1** with DDQ in dichloromethane for benzoxazole synthesis. The benzyl group in **2** was removed by a catalytic amount of Pd-C under H_2 in acetic acid. Compounds **4–6** were obtained by coupling reactions of hydroxybenzoxazole **3** with ethyl bromoacetate for **4**, G2-Br for **5**, and G3-Br for **6**, in the presence of K_2CO_3 and 18-crown-6 in refluxing dry acetone.¹⁰ The chemical structures of **4–6** were determined by 1H and ^{13}C NMR spectroscopy, UV-vis absorption spectroscopy, ESI-MS or MALDI-TOFMS spectrometry, and elemental analysis.

Steady-State Absorption and Fluorescence Studies. Figure 2 shows the steady-state UV-vis absorption spectra of **4–6** in benzene under argon at room temperature. The intensities of the bands at 300–360 nm are similar among **4–6**, and the bands are assigned to the HBO moieties, while the peaks at 280 nm, depending on the generation, are attributed to the peripheral dendrons.¹¹ Slight bathchromic shifts (2–3 nm) were observed in the absorption bands for HBO moieties in **5** and **6**, compared

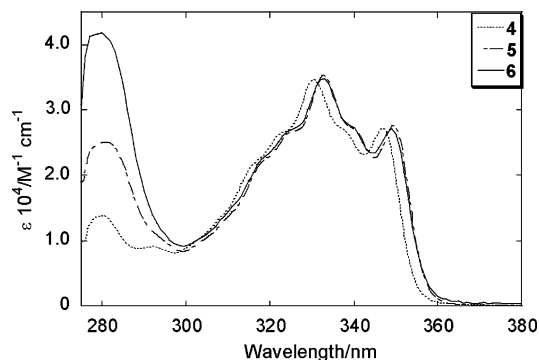


Figure 2. UV absorption spectra of HBO dendrimers **4–6** in benzene.

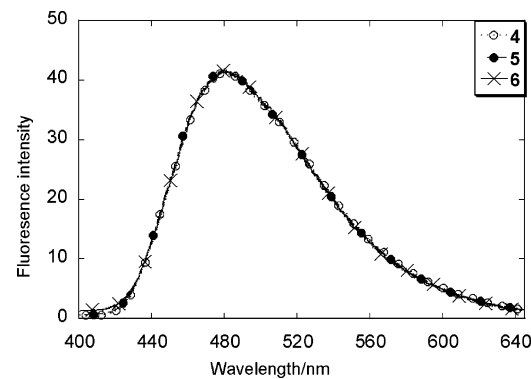


Figure 3. Fluorescence spectra ($\lambda_{ex} = 333$ nm) of HBO dendrimers **4–6** in benzene.

to **4**, suggesting a weak interaction among the chromophores in their ground states in the dendrimers. Similar absorbance shifts for the core units were also observed in poly(aryl ether) dendrimers with azobenzene or stilbene cores.¹²

The properties of the excited singlet states of **4–6** were investigated quantitatively by using steady-state fluorescence measurements. The fluorescence spectra for **4–6** in benzene under argon ($\lambda_{ex} = 333$ nm) are shown in Figure 3. The fluorescent bands with peaks at 480 nm for **4–6** having a large Stokes shift were assigned to the (*E*)-keto form in the excited singlet state ($^1K_E^*$).^{8,13} Whereas a slight difference was observed in the absorption spectra for **4** and dendrimers **5** and **6**, the fluorescence spectra among **4–6** were almost identical, indicating that there are no dendrimer effects on the energy gap between $^1K_E^*$ and 1K_E . On the other hand, the fluorescence quantum yields (Φ_f) were determined to be 0.022, 0.030, and 0.038 for **4**, **5**, and **6**, respectively, in diluted solution (10^{-6} M), increasing with increasing generation of dendrimers. Since there are four quenching pathways from $^1K_E^*$ [fluorescence emission, nonradiative decay, intersystem crossing, and isomerization to the (*Z*)-keto form (1K_Z)], the increase of the Φ_f values in higher generations suggests that there are dendrimer effects on the inhibition of the deactivation by isomerization from $^1K_E^*$ giving 1K_Z . The relation between the quantum yields of intersystem crossing (Φ_{isc}) and the production of 1K_Z by isomerization ($\Phi_{E \rightarrow Z}$) among **4–6** is mentioned later.

Transient Absorption Spectra. The transient absorption spectra of **6**, observed after laser flash excitation at 308 nm in benzene under argon, are shown in Figure 4a. This absorbance decay is composed of two components. The peak at 420 nm is not quenched by oxygen, but the peak at 560 nm is strongly affected by oxygen. Parts b and c of Figure 4 show the decay of the transient absorption at 420 and 560 nm, respectively. From the studies on HBO,^{8,14} the peak at 420 nm in Figure 4a can be assigned to 1K_Z of **6** in the ground state and the other peak is

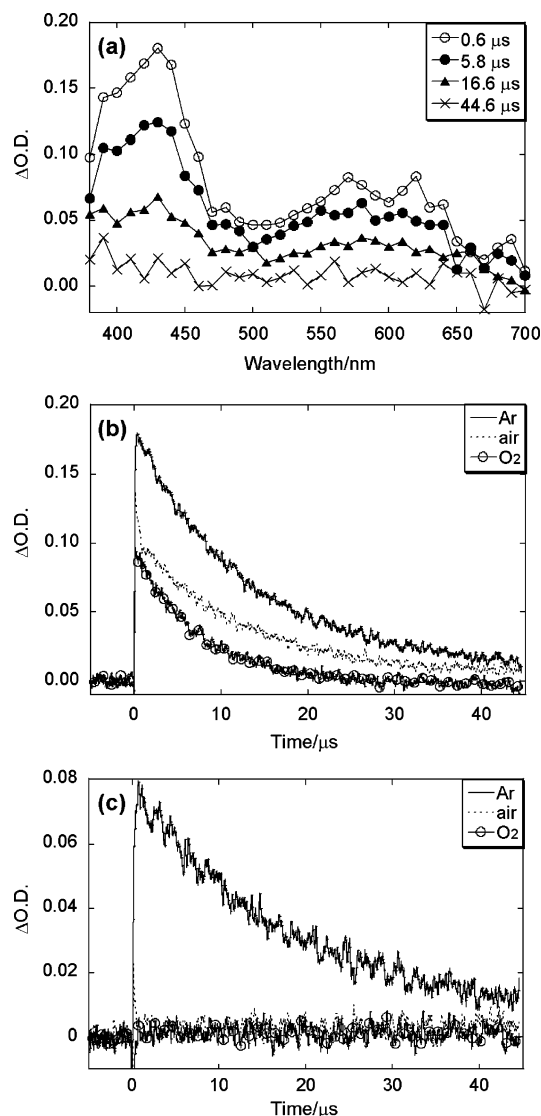


Figure 4. Transient absorption spectra of **6** on excitation at 308 nm in benzene under argon (a). Decay profiles at 420 nm for 1K_Z (b) and at 560 nm for $^3K_E^*$ (c) of **6** in benzene under argon, air, and oxygen.

TABLE 1: Lifetime of 1K_Z (τ_{KZ}), First- and Second-Order Rate Constants of 1K_Z Decay (k_1 and k_2), and Quantum Yields for Fluorescence (Φ_f), Isomerization from $^1K_E^*$ to 1K_Z (Φ_{E-Z}), Intersystem Crossing (Φ_{isc}), and Nonradiative Decay (Φ_{nr})

	$\tau_{KZ}/\mu\text{s}$	$k_1/\text{M}^{-1}\text{s}^{-1}$	$k_2/\text{M}^{-1}\text{s}^{-1}$	Φ_f	Φ_{E-Z}	Φ_{isc}	Φ_{nr}
4	3.7	74700	1.08×10^9	0.022	0.37	0.03	0.58
5	3.9	80200	7.56×10^8	0.030	0.33	0.03	0.61
6	7.9	76600	7.63×10^7	0.038	0.29	0.03	0.64

attributed to $^3K_E^*$ of **6** in the excited triplet state. These two components, 1K_Z and $^3K_E^*$, were observed in the transient absorption spectra for **4** and **5** in the same conditions. The decay curve at 420 nm could not fit the single-exponential function, but could fit the two exponential functions with first- and second-order kinetics. The half-lifetime for the 1K_Z under argon depended upon the dendrimer generation, 3.7 μs for **4**, 3.9 μs for **5**, and 7.9 μs for **6** (Table 1). This generation dependence on a re-enolization process from 1K_Z to 1E could be explained by the contribution of the bimolecular process as proposed by Grellmann et al.;¹⁵ the metastable 1K_Z of HBO decays to 1E partly in a second-order reaction or in a bimolecular reaction by double proton transfer as in the case of HBT and HBC (Figure 5). The generation dependence of the lifetimes of 1K_Z

suggests that the isomerization from 1K_Z to 1K_E followed by an ultrafast re-enolization process takes place in mixed first- and second-order reactions and the second-order reaction in higher generation dendrimers is inhibited by bulky dendrons. Thus, we further investigated the isomerization from 1K_Z to 1K_E by determination of the lifetime at different laser powers. We will describe this process simply as a re-enolization reaction.

Determination of the Quantum Yields of Formation of the *trans*-Keto Form. The quantum yields of formation of 1K_Z (Φ_{E-Z}) for **4–6** can be estimated in benzene by comparing the ΔOD values of 1K_Z of **4–6** with that of the T–T absorption of an optically matched benzophenone ($\epsilon(530\text{ nm}) = 7220\text{ M}^{-1}\text{ cm}^{-1}$) solution at 308 nm. The molar extinction coefficients for 1K_Z of **4–6** at 420 nm were assumed to be the same as that of (*Z*)-NBT ($\epsilon(420\text{ nm}) = 7000$).¹⁶ Thus, the Φ_{E-Z} values were estimated to be 0.37, 0.33, and 0.29 for **4**, **5**, and **6**, respectively, which decreased with increasing generation. The results indicate that the increase of the fluorescence quantum yields for **4–6** in higher generations is due to the suppression of isomerization from $^1K_E^*$ to 1K_Z by peripheral dendrons.

Determination of the Rate Constants for a Re-enolization Reaction. To determine the rate constants for the isomerization from 1K_Z to 1K_E followed by a re-enolization reaction, the peak intensity of the transient species changes at different laser powers. The higher the laser power, the higher the second-order component of 1K_Z decay. It is possible to determine a second-order rate constant (k_2) for a bimolecular reaction by double proton transfer defined as the slope of the straight line obtained by plotting the initial observed rate constant of 1K_Z decay against the initial concentration of 1K_Z ($[M]_0$) (eq 1),¹⁷ where $[M]$ is

$$-\frac{d}{dt}\ln[M]_{\text{initial}} = k_1 + k_2[M]_0 \quad (1)$$

the concentration of 1K_Z , $[M]_0$ is the initial concentration of 1K_Z , k_1 is the pseudo-first-order rate constant, and k_2 is the second-order rate constant. Since $[M] = \Delta\text{OD}/\epsilon$, eq 2 can be

$$-\frac{d}{dt}\ln(\Delta\text{OD}) = k_1 + \frac{k_2}{\epsilon}(\Delta\text{OD})_0 \quad (2)$$

given. Thus, the first- and second-order rate constants k_1 and k_2 were obtained; $k_1 = 74700\text{ s}^{-1}$ and $k_2 = 1.08 \times 10^9\text{ M}^{-1}\text{ s}^{-1}$ for **4**, $k_1 = 80200\text{ s}^{-1}$ and $k_2 = 7.56 \times 10^8\text{ M}^{-1}\text{ s}^{-1}$ for **5**, and $k_1 = 76600\text{ s}^{-1}$ and $k_2 = 7.63 \times 10^7\text{ M}^{-1}\text{ s}^{-1}$ for **6**. The k_2 value for the small molecule **4** is on the same order as the diffusion-controlled rate constant ($6.3 \times 10^9\text{ M}^{-1}\text{ s}^{-1}$). The first-order rate constants (k_1) were almost generation independent. On the other hand, the bimolecular reaction is highly suppressed with increasing generations, probably because the dendrimer structure disturbs the bimolecular reaction at the core unit. One can say that this result is the typical dendrimer effect on the isolation of the core from the outside.¹⁸ This inhibition effect on the contribution of the bimolecular re-enolization reaction should correlate to increase the lifetime of 1K_Z in higher generations.

Determination of the Quantum Yields of Intersystem Crossing and Nonradiative Decay. The quantum yields for intersystem crossing (Φ_{isc}) for **4–6** can be estimated by the triplet–triplet energy transfer from **4–6** to β -carotene with an optically matched reference HBO ($\Phi_{isc} = 0.03$) solution at 308 nm. β -Carotene absorbs light at 308 nm, but did not produce any transient species upon excitation at 308 nm on the microsecond time scale. Therefore, one can estimate the Φ_{isc}

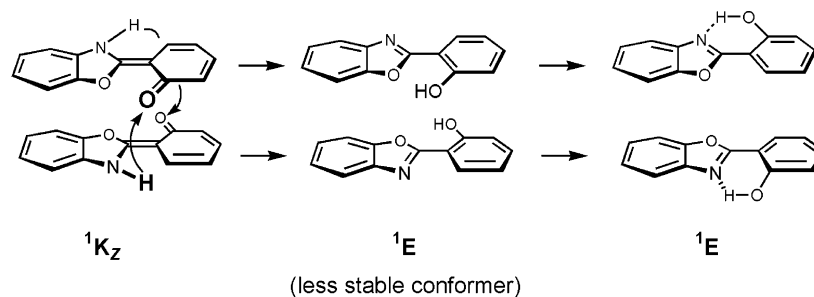


Figure 5. Proposed bimolecular process for reverse tautomerization from 1K_Z to 1E .

values by observing the intensity of T–T absorption spectra at 540 nm. The estimated values of the quantum yields of intersystem crossing (Φ_{isc}) were 0.03 for 4–6, which were the same as that for HBO and were generation independent. The low quantum yields of intersystem crossing and the high quantum yields of isomerization for 4–6 give a clear indication that the photoisomerization proceeds in the excited singlet state from ${}^1K_E^*$ to 1K_Z .

There are four relaxation pathways from ${}^1K_E^*$: (1) fluorescence emission, (2) photoisomerization, (3) intersystem crossing, and (4) nonradiative decay. Since we have estimated the values of Φ_f , Φ_{E-Z} , and Φ_{isc} for 4–6, the quantum yield for nonradiative decay (Φ_{nr}) can be calculated to be 0.58, 0.61, and 0.64, for 4, 5, and 6, respectively, increasing in higher generations. This result correlates well with the decrease in isomerization efficiency (Φ_{E-Z}) in higher generations. In a previous study,^{12a,19} we have reported that the isomerization efficiency in the stilbene dendrimers in organic solvents was generation independent, probably because there are two different competing isomerization modes for stilbenes, one-bond flip (OBF) and hula-twist (HT) mechanisms. When the isomerization with the OBF mechanism is inhibited by bulky dendrons, another isomerization mechanism (HT) can be operative, resulting in similar isomerization efficiencies.²⁰ Liu et al. proposed that a H atom is needed on the C=C double bond to induce HT isomerization.²¹ Unlike stilbenes, ${}^1K_E^*$ of HBO has no H atom at the double bond and therefore may undergo isomerization only with the OBF mechanism, which requires a larger volume change compared to the HT mechanism, especially in the molecules with bulky substituent groups. Therefore, the isomerization efficiency in HBO decreased with increasing dendrimer generation, which resulted in the enhancement of both nonradiative decay and fluorescence quantum yields in higher generations.

Potential Energy Diagram. The potential energy diagram of 4–6 is summarized in Figure 6. At room temperature 4–6 exist as 1E . On photoirradiation, ${}^1K_E^*$ is produced through the ESIPT process from ${}^1E^*$. The produced ${}^1K_E^*$ gave large Stokes-shifted fluorescence at 450–500 nm, underwent intersystem crossing to ${}^3K_E^*$, or isomerized to 1K_Z . The metastable 1K_Z underwent the isomerization to 1K_E followed by an ultrafast re-enolization process to 1E . Most interestingly, the efficiency of the large Stokes-shifted fluorescence from the ESIPT molecule could be increased by the introduction of a dendrimer structure, probably because the bulky dendrons inhibited the isomerization efficiency. Furthermore, the determination of the rate constants for the re-enolization process revealed that the process was mixed first- and second-order reactions. The mechanism of the first-order reaction may be OBF isomerization, and that of the second-order reaction may involve bimolecular proton exchange. In higher generations, the second-order reaction was suppressed by dendrons whereas the first-order rate constants (k_1) were

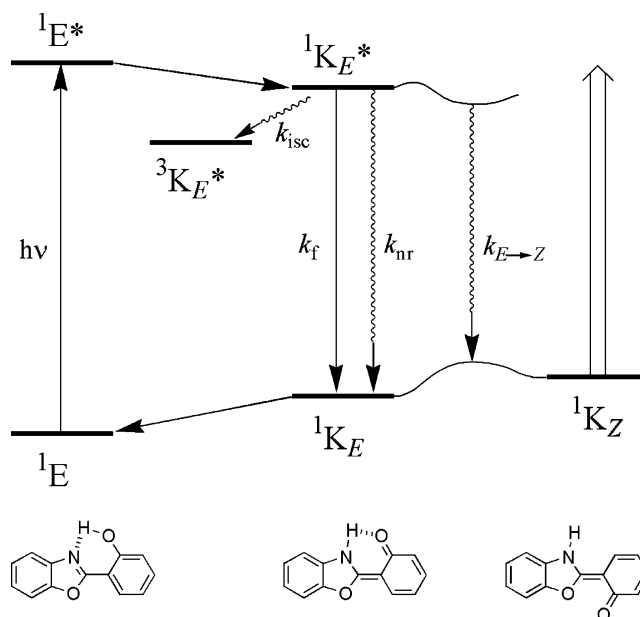


Figure 6. Potential energy diagram for forward hydrogen atom transfer in the excited state (${}^1E^* \rightarrow {}^1K_E^*$) followed by deactivation with isomerization from ${}^1K_E^*$ to 1K_Z and reverse tautomerization from 1K_Z to 1E by way of unimolecular reverse thermal isomerization from 1K_Z to 1K_E .

generation independent. The fluorescence spectra were almost identical among 4–6, indicating the energy gaps between 1K_E and ${}^1K_E^*$ in 4–6 were almost the same.

Conclusion

The photochemistry and photophysics of dendrimer molecules have been studied. Among those, the dendrimer effect on fluorescence spectroscopy, energy transfer, electron transfer, and hole transfer have been reported. As far as we are aware, there are few reports of the dendrimer effect on photochemical processes such as the isomerization efficiency. The present results of the dendrimer effect on the fluorescence quantum yield of the excited-state intermediate are the first clear evidence of an efficiency increase with relation to the deactivation process of ${}^1K_E^*$ by isomerization to give the ground-state 1K_Z . Furthermore, the surrounding dendron affects the reverse tautomerization process by suppressing the bimolecular reaction.

Acknowledgment. This work was supported by a Grant-in-Aid for Scientific Research on Priority Areas (417), a Grant-in-Aid for Scientific Research (16350005) and the 21st Century COE Program from the Ministry of Education, Culture, Sports, Science and Technology (MEXT) of the Japanese Government, University of Tsukuba Research Projects, Asahi Glass Foundation, and JSR Corp.

References and Notes

- (1) (a) Henary, M. M.; Fahrini, C. J. *J. Phys. Chem. A* **2002**, *106*, 5210–5220. (b) Tanaka, K.; Kumagai, T.; Aoki, H.; Deguchi, M.; Iwata, S. *J. Org. Chem.* **2001**, *66*, 7328–7333. (c) Ohshima, A.; Momotake, A.; Arai, T. *Tetrahedron Lett.* **2004**, *45*, 9377–9381. (d) Sytnik, A.; Delvalle, J. C. *J. Phys. Chem.* **1995**, *99*, 13028–13032. (e) Sytnik, A.; Kasha, M. *Proc. Natl. Acad. Sci. U.S.A.* **1994**, *91*, 8627–8630. (f) Sytnik, A.; Gormin, D.; Kasha, M. *Proc. Natl. Acad. Sci. U.S.A.* **1994**, *91*, 11968–11972.
- (2) (a) Chou, P. T.; Martinez, M. L.; Clements, J. H. *Chem. Phys. Lett.* **1993**, *204*, 395–399. (b) Parthenopoulos, D. A.; McMorro, D.; Kasha, M. *J. Phys. Chem.* **1991**, *95*, 2668–2674.
- (3) (a) O'Connor, D. B.; Scott, G. W.; Coulter, D. R.; Yavrouian, A. *J. Phys. Chem.* **1991**, *95*, 10252–10261. (b) Keck, J.; Kramer, H. E. A.; Port, H.; Hirsch, T.; Fischer, P.; Rytz, G. *J. Phys. Chem.* **1996**, *100*, 14468–14475.
- (4) (a) Fournier, T.; Pommeret, S.; Mialocq, J.-C.; Deflandre, A.; Rozot, R. *Chem. Phys. Lett.* **2000**, *325*, 1671–175. (b) Arzhantsev, S. Y.; Takeuchi, S.; Tahara, T. *Chem. Phys. Lett.* **2000**, *330*, 83–90. (c) Chou, P. T.; Chen, Y.-C.; Yu, W.-S.; Chou, Y.-H.; Wei, C.-Y.; Cheng, Y.-M. *J. Phys. Chem. A* **2001**, *105*, 1731–1740. (d) Ernsting, N. P.; Kovalenko, S. A.; Senyushkina, T.; Saam, J.; Farztdinov, V. *J. Phys. Chem. A* **2001**, *105*, 3443–3453. (e) Mitra, S.; Tamai, N. *Phys. Chem. Chem. Phys.* **2003**, *5*, 4647–4652. (f) Abou-Zied, O. K.; Jimenez, R.; Thompson, E. H. Z.; Millar, D. P.; Romesberg, F. E. *J. Phys. Chem. A* **2002**, *106*, 3665–3672. (g) Okabe, C.; Nakabayashi, T.; Inokuchi, Y.; Nishi, N.; Sekiya, H. *J. Chem. Phys.* **2004**, *121*, 9436–9442. (h) Chou, P. T.; Pu, S.-C.; Cheng, Y.-M.; Yu, W.-S.; Yu, Y.-C.; Hung, F.-T.; Hu, W.-P. *J. Phys. Chem. A* **2005**, *109*, 3777–3787.
- (5) (a) Nagaoka, S.; Kusunoki, J.; Fujibuchi, T.; Hatakenaka, S.; Mukai, K.; Nagashima, U. *J. Photochem. Photobiol., A* **1999**, *122*, 151–159. (b) Ohshima, A.; Momotake, A.; Arai, T. *J. Photochem. Photobiol., A* **2004**, *162*, 473–479.
- (6) (a) Ziótek, M.; Kubicki, J.; Maciejewski, A.; Naskręcki, R.; Grabowska, A. *Chem. Phys. Lett.* **2003**, *369*, 80–89. (b) Balamurai, M. M.; Dogra, S. K. *Chem. Phys.* **2004**, *305*, 95–103. (c) LeGourriec, D.; Kharlanov, V.; Brown, R. G.; Rettig, W. *J. Photochem. Photobiol., A* **1998**, *117*, 209–216.
- (7) Kim, S.; Chang, D. W.; Park, S. Y.; Kawai, H.; Nagamura, T. *Macromolecules* **2002**, *35*, 2748–2753.
- (8) (a) Seo, J.; Kim, S.; Park, S. Y. *J. Am. Chem. Soc.* **2004**, *126*, 11154–11155. (b) Ogawa, A. K.; Abou-Zied, O. K.; Tsui, V.; Jimenez, R.; Case, D. A.; Romesberg, F. E. *J. Am. Chem. Soc.* **2000**, *122*, 9917–9920. (c) Wang, H.; Zhang, H.; Abou-Zied, O. K.; Yu, C.; Romesberg, F. E.; Glasbeek, M. *Chem. Phys. Lett.* **2003**, *367*, 599–608. (d) Yang, G.; Morlet-Savary, F.; Peng, Z.; Wu, S.; Fouassier, J.-P. *Chem. Phys. Lett.* **1996**, *256*, 536–542. (e) Tanaka, K.; Deguchi, M.; Yamaguchi, S.; Yamada, K.; Iwata, S. *J. Heterocycl. Chem.* **2001**, *38*, 131–136.
- (9) Gryniewicz, G.; Poenie, M.; Tsien, R. Y. *J. Biol. Chem.* **1985**, *260*, 3440–3450.
- (10) Hawker, C. J.; Wooley, K. L.; Fréchet, J. M. *J. Chem. Soc., Perkin Trans. 1* **1993**, 1287–1297.
- (11) (a) Hayakawa, J.; Momotake, A.; Arai, T. *Chem. Commun.* **2003**, 94–95. (b) Uda, M.; Mizutani, T.; Hayakawa, J.; Momotake, A.; Ikegami, M.; Nagahata, R.; Arai, T. *Photochem. Photobiol.* **2002**, *76*, 596–605.
- (12) (a) Momotake, A.; Hayakawa, J.; Nagahata, R.; Arai, T. *Bull. Chem. Soc. Jpn.* **2004**, *77*, 1195–1200. (b) Momotake, A.; Arai, T. *Tetrahedron Lett.* **2004**, *45*, 4131–4134.
- (13) (a) Hillebrand, S.; Segala, M.; Buckup, T.; Correia, R. R. B.; Horowitz, F.; Stefani, V. *Chem. Phys.* **2001**, *273*, 1–10. (b) Tong, H.; Zhou, G.; Wang, L.; Jing, X.; Wang, F.; Zhang, J. *Tetrahedron Lett.* **2003**, *44*, 131–134.
- (14) Itoh, M.; Fujiwara, Y. *J. Am. Chem. Soc.* **1985**, *107*, 1561–1565.
- (15) Stephan, J. S.; Grellmann, K. H. *J. Phys. Chem.* **1995**, *99*, 10066–10068.
- (16) Ikegami, M.; Arai, T. *J. Chem. Soc., Perkin Trans. 2* **2002**, 1296–1301.
- (17) Bensasson, R. V.; Gramain, J.-C. *J. Chem. Soc., Faraday Trans. 1* **1980**, *76*, 1801–1810.
- (18) (a) Ueyama, M.; Aida, T. *J. Am. Chem. Soc.* **2002**, *124*, 11392–11403. (b) Tomoyose, Y.; Diang, D.-L.; Jin, R.-H.; Aida, T.; Yamashita, T.; Horie, K. *Macromolecules* **1996**, *29*, 5236–5238. (c) Bhyrappa, P.; Young, J. K.; Moore, J. S.; Suslick, K. S. *J. Am. Chem. Soc.* **1996**, *118*, 5708–5711.
- (19) Uda, M.; Momotake, A.; Arai, T. *Org. Biomol. Chem.* **2003**, *1*, 1635–1637.
- (20) Uda, M.; Momotake, A.; Arai, T. *Tetrahedron Lett.* **2005**, *46*, 3021–3024.
- (21) (a) Liu, R. S. H.; Asato, A. E. *Proc. Natl. Acad. Sci. U.S.A.* **1985**, *82*, 259–263. (b) Liu, R. S. H.; Hammond, G. S. *Proc. Natl. Acad. Sci. U.S.A.* **2000**, *97*, 11153–11158. (c) Liu, R. S. H.; Hammond, G. S. *Chem.—Eur. J.* **2001**, *7*, 4536–4544. (d) Liu, R. S. H. *Acc. Chem. Res.* **2001**, *34*, 555–562.